

Supplementary Information

Monodisperse PdSn/SnO_x core/shell nanoparticles with superior electrocatalytic ethanol oxidation performance

**Qiang Gao,^a Tianyou Mou,^a Shikai Liu,^b Grayson Johnson,^c Xue Han,^a Zihao Yan,^a
Mengxia Ji,^a Qian He,^b Sen Zhang,^c Hongliang Xin,^{*a} and Huiyuan Zhu^{*a}**

^aDepartment of Chemical Engineering, Virginia Polytechnic Institute and State University, 635 Prices Fork Rd., Blacksburg, Virginia 24061, USA

^bDepartment of Materials Science and Engineering, National University of Singapore, 9 Engineering Drive 1, 117575, Singapore

^cDepartment of Chemistry, University of Virginia, Charlottesville, Virginia 22904, USA.

*To whom correspondence should be addressed. E-mail: hxin@vt.edu or huiyuanz@vt.edu

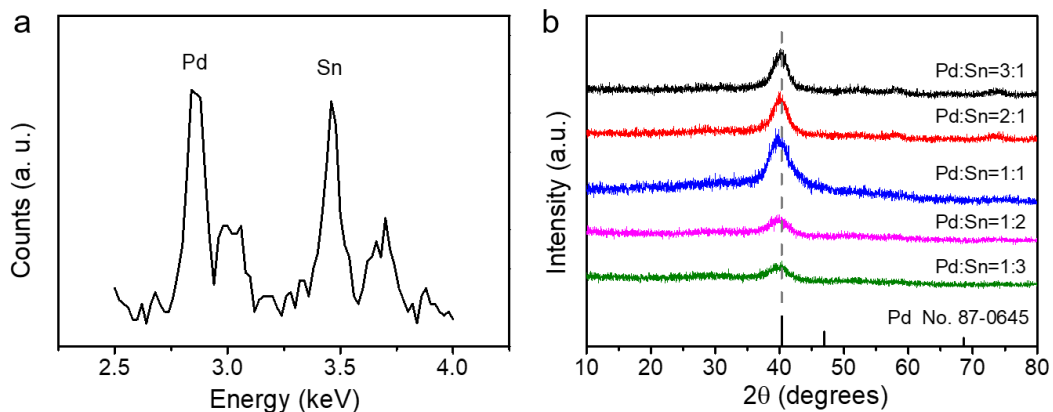


Fig. S1. (a) X-EDS spectra of PdSn/SnO_x core/shell nanoparticles. (b) XRD patterns of PdSn/SnO_x core/shell nanoparticles with different Pd/Sn ratios.

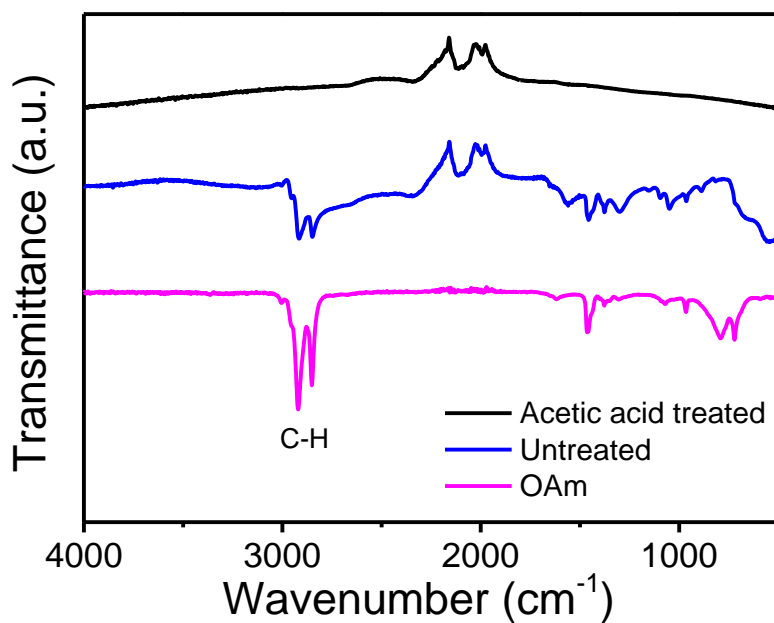


Fig. S2. FTIR spectra of OAm and PdSn/SnO_x nanoparticles before and after ligand removal.

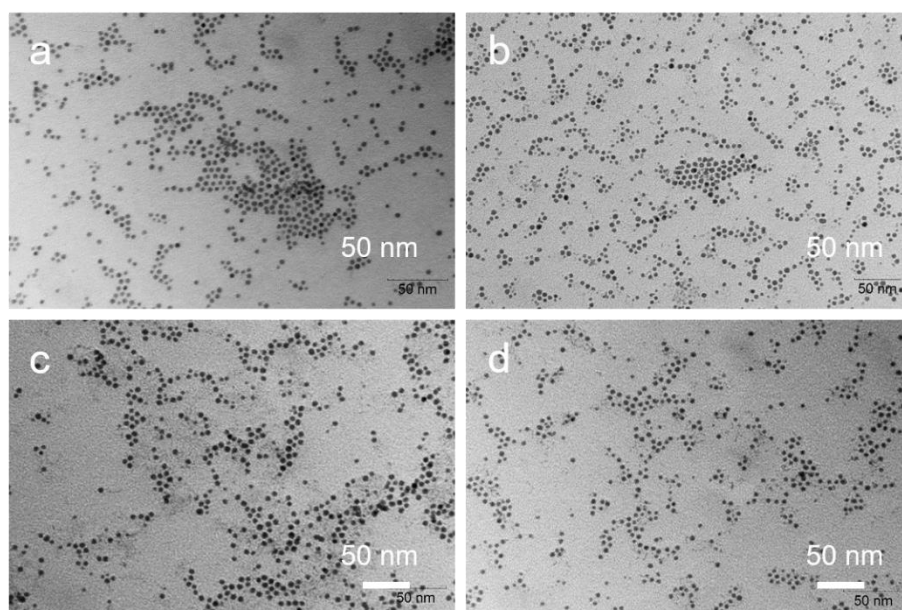


Fig. S3. TEM images of the samples obtained with different molar ratio of Pd/Sn: (a) 3:1; (b) 2:1; (c) 1:2 and (d) 1:3.

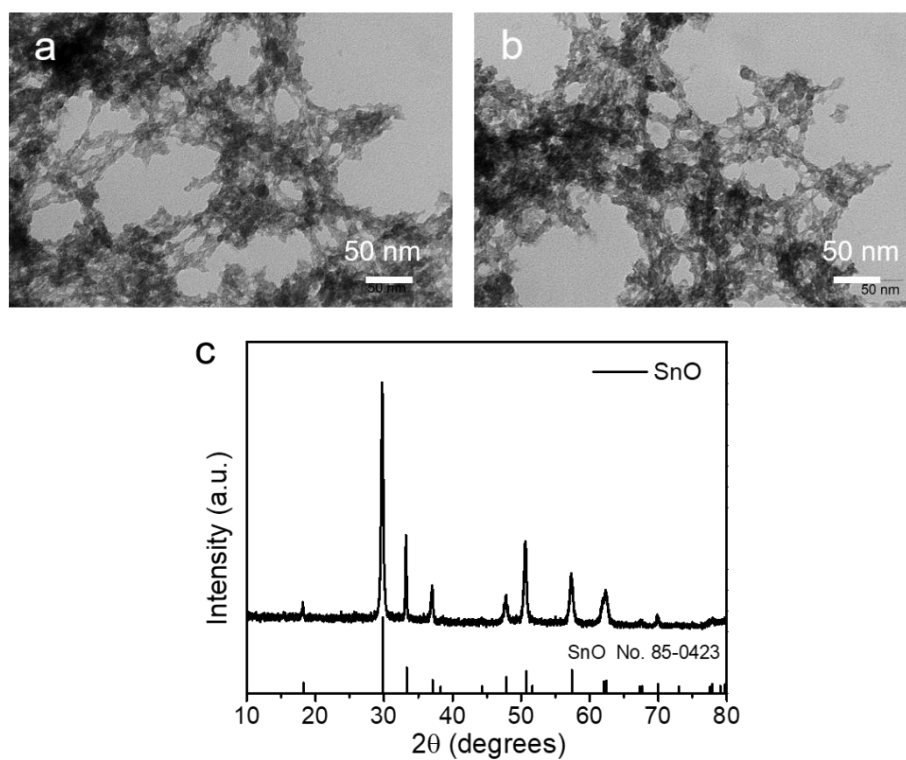


Fig. S4. (a, b) TEM images and (c) the XRD pattern of SnO aggregates.

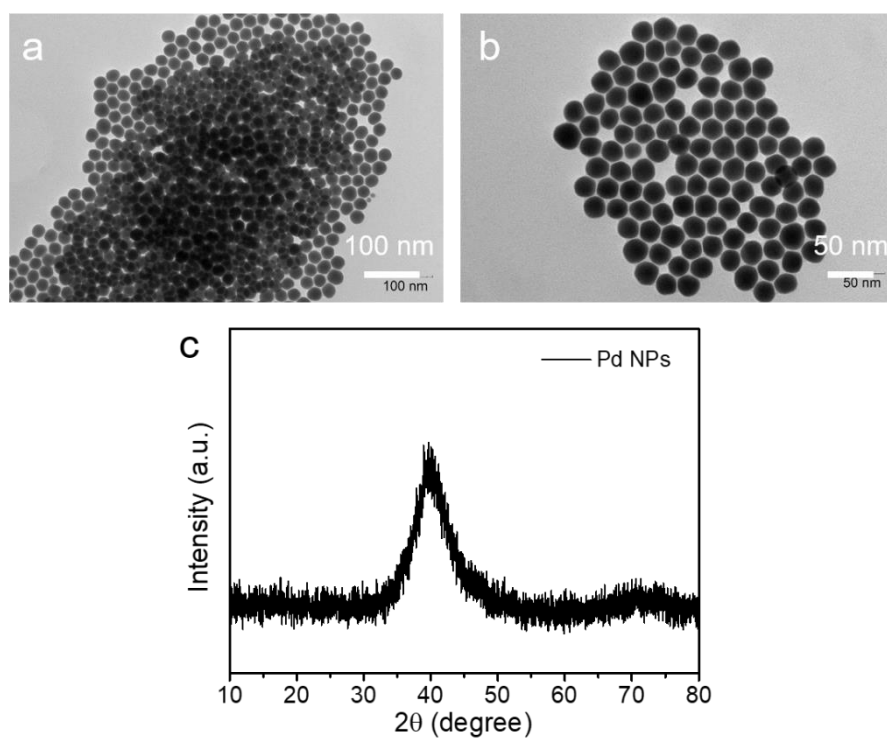


Fig. S5. (a, b) TEM images and (c) the XRD pattern of Pd nanoparticles.

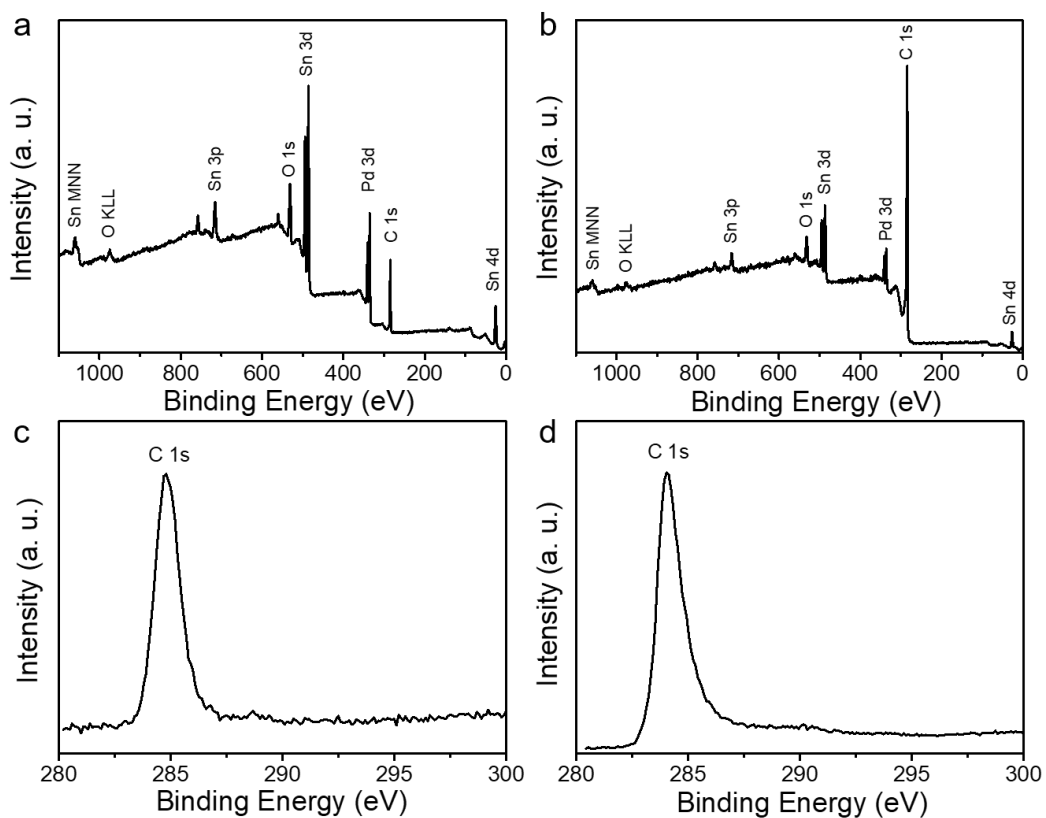


Fig. S6. XPS survey spectra of (a) as-synthesized PdSn/SnO_x nanoparticles and (b) acetic acid treated C-PdSn/SnO_x nanoparticles. High-resolution C1s spectra of (c) as-synthesized PdSn/SnO_x nanoparticles and (d) acetic acid treated C-PdSn/SnO_x nanoparticles.

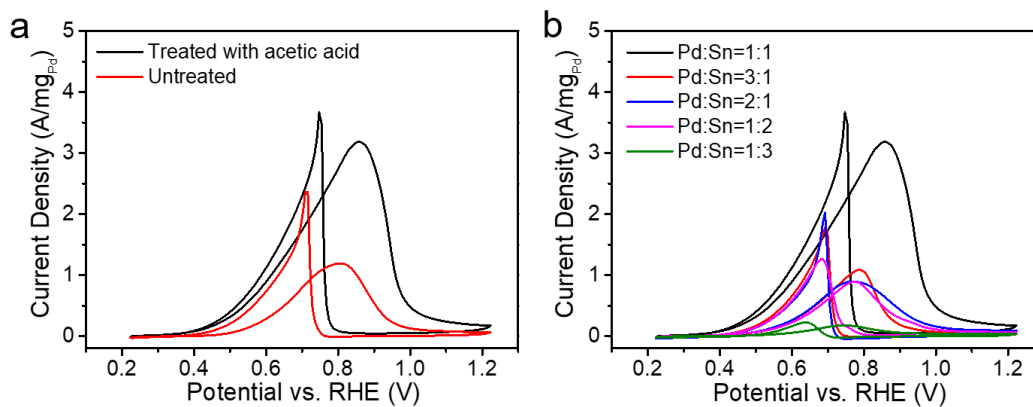


Fig. S7. (a) CV curves of ethanol oxidation for as-synthesized untreated PdSn/SnO_x nanoparticles and acetic acid treated C-PdSn/SnO_x catalyst in 1 M KOH+1 M ethanol. (b) EOR activities of the C-PdSn/SnO_x catalysts with different Pd/Sn ratios.

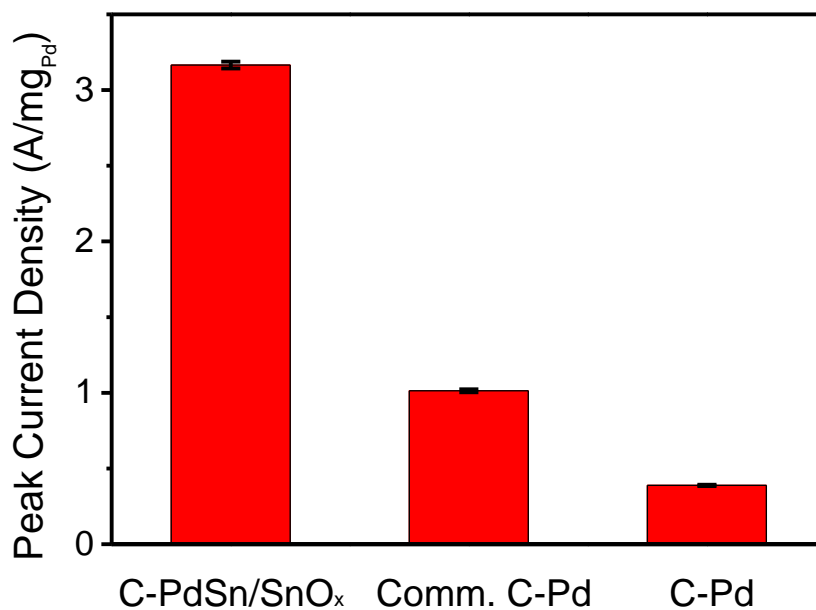


Fig. S8. The mass peak current density of C-PdSn/SnO_x, C-Pd, and commercial C-Pd catalysts. The error bars correspond to the standard deviation of three independent measurements.

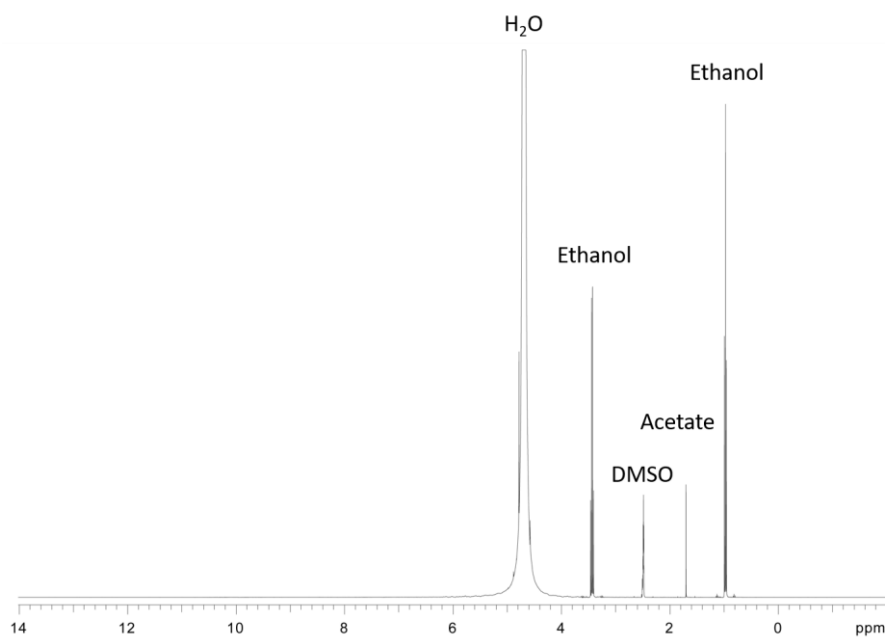


Fig. S9. Representative NMR spectra of the electrolyte after 12h ethanol oxidation electrolysis at 0.824 V vs. RHE for C-PdSn/SnO_x.

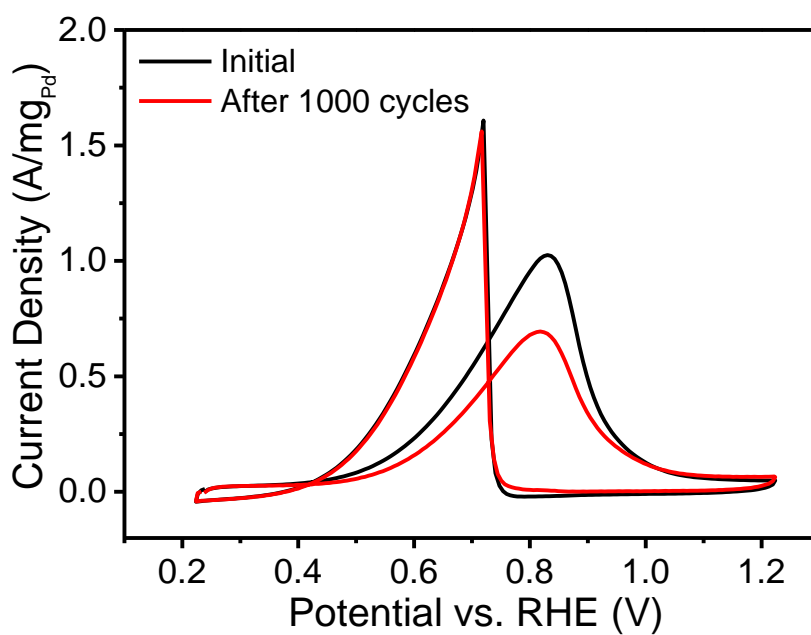


Fig. S10. EOR polarization curves of commercial C-Pd catalyst before and after 1000 cycles of accelerated stability tests.

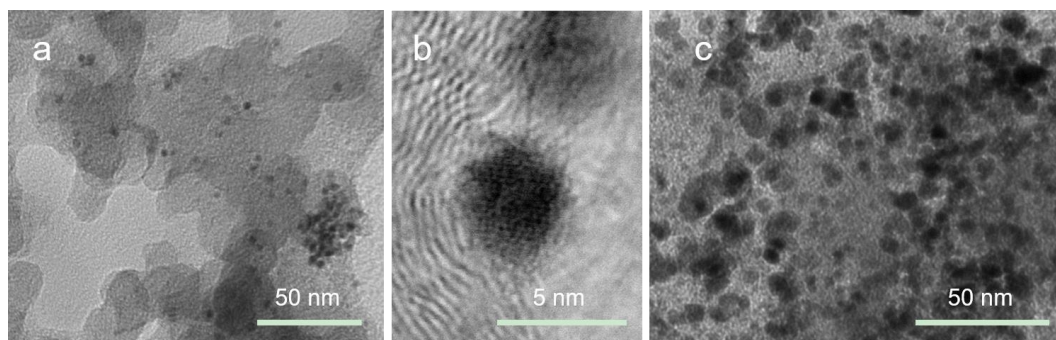


Fig. S11. (a) A lower magnification TEM image and (b) a HRTEM image of C-PdSn/SnO_x after durability test. (c) Commercial C-Pd after durability test.

Table S1. Compositions of untreated PdSn/SnO_x nanoparticles and acetic acid treated C-PdSn/SnO_x catalyst according to XPS analysis.

Sample	Pd	Sn
Untreated	35.45	64.55
Acetic acid treated	38.78	61.22

Table S2. The ratio of Sn⁰ and Sn⁴⁺ in untreated PdSn/SnO_x nanoparticles and acetic acid treated C-PdSn/SnO_x catalyst according to XPS analysis.

Sample	Sn ⁰	Sn ⁴⁺
Untreated	26.09	73.91
Acetic acid treated	33.81	66.19

Table S3. Comparison of the activity of various Pd-based nanomaterials for EOR in alkaline media.

Catalyst	Loading ($\mu\text{g}/\text{cm}^2$)	Mass activity ($\text{A}/\text{mg}_{\text{Pd}}$)	Ref.
C-PdSn/SnO_x	25	3.2	This work
Commercial C-Pd	25	1.0	This work
Pd-Sn Alloy dendrites	196	0.576	Ref. ¹
Pd ₂ Sn nanorods	N/A	0.447	Ref. ²
Intermetallic Pd ₂ Sn/C	12.85	0.987	Ref. ³
Pd ₈₆ Sn ₁₄ /C	N/A	1.3	Ref. ⁴
PdSn-SnO ₂ /C	160	0.429	Ref. ⁵
Pd/SnO ₂ -graphene	180	0.256	Ref. ⁶
PdCo nanotube	23.4	1.5	Ref. ⁷
PdNi Hollow Nanospheres	20	3.63	Ref. ⁸
Pd-NiCoO _x /C	N/A	0.43	Ref. ⁹
Pd/Ni(OH) ₂ /rGO	145	1.546	Ref. ¹⁰
Flower-like ordered Pd ₃ Pb	N/A	0.51	Ref. ¹¹
Pd ₃ Pb Nanocubes	2.5	4.4	Ref. ¹²
Pd ₇ /Ru ₁ nanodendrites	56.62	1.15	Ref. ¹³
PdPt nanowires	71.4	0.94	Ref. ¹⁴
Pd ₄₀ Ni ₄₃ P ₁₇ /C	22.57	4.945	Ref. ¹⁵
Ordered PdCuNi/C	26.02	6.17	Ref. ¹⁶
Ordered PdCuCo/C	26.02	7.72	Ref. ¹⁶

Models and Computational Details

All density functional theory (DFT) calculations were performed using Vienna Ab initio Simulation Package (VASP),¹⁷⁻¹⁹ interfaced with the Atomic Simulation Environment.^{20, 21} In this work, 3 model systems including pure Pd metal, Pd₃Sn alloy, and Pd₃Sn alloy with SnO_x clusters (Pd₃Sn/SnO_x) were used. For the pure Pd metal surface, Pd (111) was chosen and represented by three layers of 4 × 4 surface cells with a lattice parameter of 3.957 Å, shown in Fig. S12a. For the Pd₃Sn alloy surface, Pd₃Sn (111) was chosen with the face centered cubic (*fcc*) crystal structure. Lattice constant 4.040 Å was obtained by optimizing Pd₃Sn bulk structure. For the Pd₃Sn/SnO_x surface, a slab from the previous case was employed with a SnO₂ cluster adsorbed on the Pd₃Sn surface, resembling the Pd₃Sn/SnO_x interface (Fig. S12). The slab was separated with 15 Å of vacuum space to eliminate interactions between periodic images.

The Perdew-Burke-Ernzerhof generalized gradient approximation combined with DFT-D3 corrections was selected as the description of exchange and correlation as the consideration of van der Waals interactions. The adsorbates and top two layers were fully relaxed until the interatomic forces are minimized down to 0.03 eV/Å, while the bottom layer was fixed in their bulk positions. A 3 × 3 × 1 k-point mesh was used using the method developed by Monkhorst and Pack.²² The cut-off energy was 400 eV for plane-wave basis sets. The atomic cores were described by ultrasoft pseudopotentials. The occupation of Kohn-Sham eigenstates was smeared by the Methfessel-Paxton function with a width of 0.2 eV to speed up the convergence for model systems, and all energies were evaluated by extrapolating to 0 K. Free formation energies of all adsorbed species are referenced to gas phase molecules. All values provided in this work are Gibbs free energies corrected by ZPE, entropy effect, gas phase correction and solvation effect which are provided in Table S4. Values are in consistent with other literature values.²³⁻²⁵

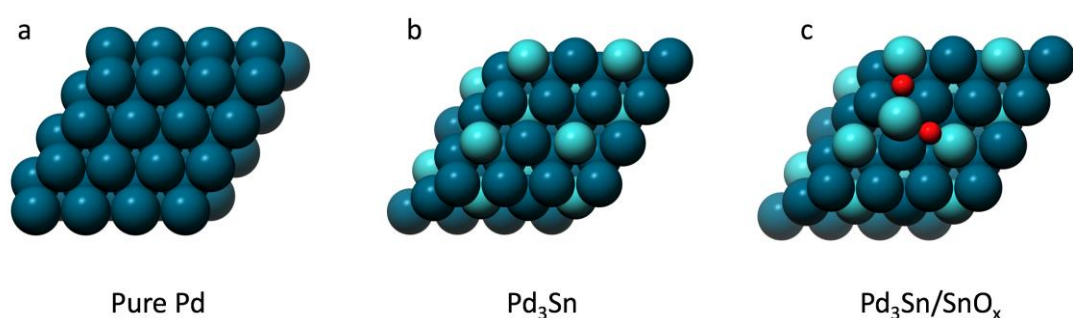


Fig. S12. (a) Pure Pd (111) surface. (b) Pd₃Sn (111) alloy surface. (c) Pd₃Sn (111) alloy with a SnO₂ cluster on surface.

Table S4. Thermodynamics of free molecules and surface species^a

Molecules	ZPE	-TS	Gas phase correction	Solvation
CO(g)	0.13	-0.67	-0.20	-
H ₂ (g)	0.27	-0.42	-	-
H ₂ O(l)	0.58	-0.57	-	-0.09
CH ₃ CH ₂ OH(aq)	2.12	-0.913	-0.05	-0.17
CH ₃ COOH(aq)	1.63	-0.88	0.13	-0.16
*CH ₃ CO	1.24	-0.21		-0.1
*CH ₃ COOH	1.66	-0.3		-0.25
*OH (top)	0.33	-0.1		-0.5
*OH (fcc)	0.33	-0.11		-0.5
*OH (brg)	0.36	-0.09		-0.5
*CH ₃ CO+*OH (TS)	1.6	-0.3		-0.35

^aAll values are in electronvolt (eV). Temperature was set to 298.15K.

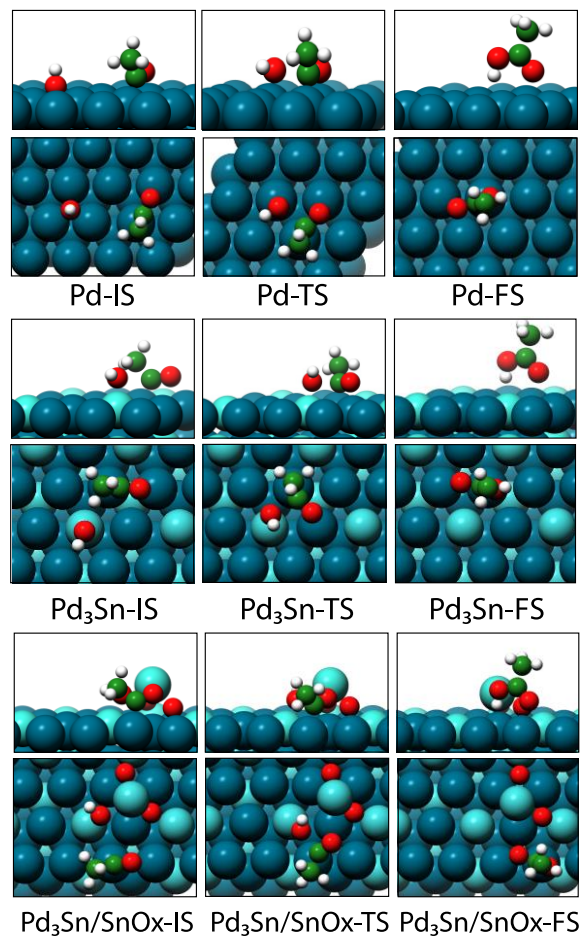
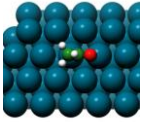
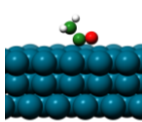
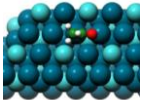
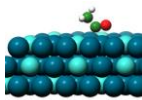
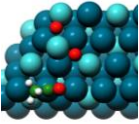
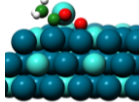
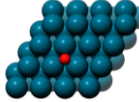
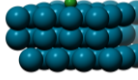
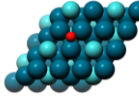
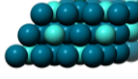
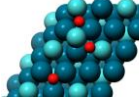
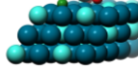


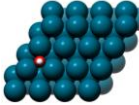
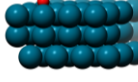
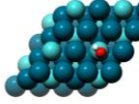
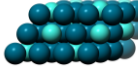
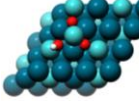
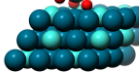
Fig. S13. The CH₃CO-OH coupling step on Pd (111), Pd₃Sn (111) and Pd₃Sn/SnO_x (111) surfaces with top and side views.

Table S5. Most stable adsorption sites of various adsorbates on different surfaces

Surfaces	*CH ₃ CO			
	ΔG (eV)	Site	Top View	Side View
Pd	-1.78	Double top Pd		
Pd ₃ Sn	-1.18	Double top Pd		

Pd ₃ Sn/SnO _x	-1.2	Double top Pd		
-------------------------------------	------	---------------	--	---

Surfaces	*CO			
	ΔG (eV)	Site	Top View	Side View
Pd	-1.90	Hol (fcc)		
Pd ₃ Sn	-1.53	Hol (hcp)		
Pd ₃ Sn/SnO _x	-1.53	Hol (hcp)		

Surfaces	*OH			
	ΔG (eV)	Site	Top View	Side View
Pd	0.015	Hol (fcc)		
Pd ₃ Sn	-0.03	Top (Sn)		
Pd ₃ Sn/SnO _x	-0.07	Sn-Sn Brg		

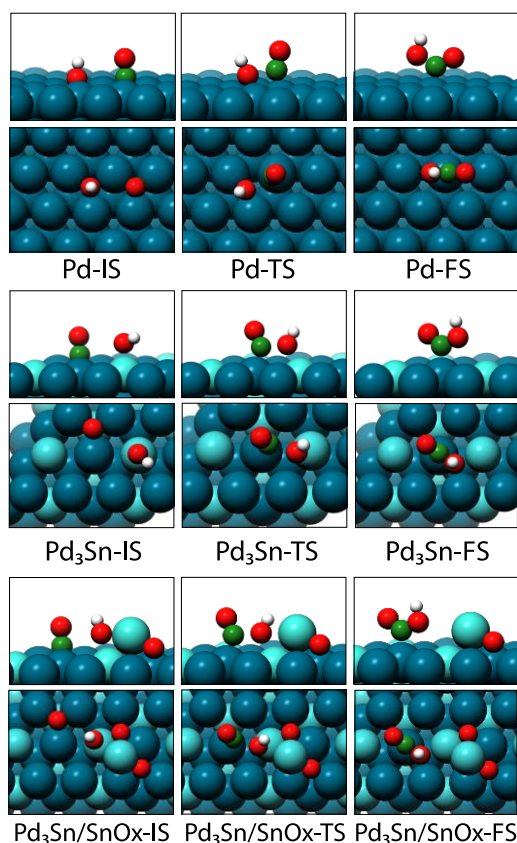


Fig. S14. The CO-OH coupling step on Pd (111), Pd₃Sn (111) and Pd₃Sn/SnO_x (111) surfaces with top and side views.

Reference:

1. L.-X. Ding, A.-L. Wang, Y.-N. Ou, Q. Li, R. Guo, W.-X. Zhao, Y.-X. Tong and G.-R. Li, *Sci. Rep.*, 2013, **3**, 1181.
2. Z. Luo, J. Lu, C. Flox, R. Nafria, A. Genç, J. Arbiol, J. Llorca, M. Ibáñez, J. R. Morante and A. Cabot, *J. Mater. Chem. A*, 2016, **4**, 16706-16713.
3. C. Wang, Y. Wu, X. Wang, L. Zou, Z. Zou and H. Yang, *Electrochim. Acta*, 2016, **220**, 628-634.
4. W. Du, K. E. Mackenzie, D. F. Milano, N. A. Deskins, D. Su and X. Teng, *Acs Catal.*, 2012, **2**, 287-297.
5. H. Mao, L. Wang, P. Zhu, Q. Xu and Q. Li, *Int. J. Hydrog. Energy*, 2014, **39**, 17583-17588.
6. Z. Wen, S. Yang, Y. Liang, W. He, H. Tong, L. Hao, X. Zhang and Q. Song, *Electrochim. Acta*, 2010, **56**, 139-144.
7. A.-L. Wang, X.-J. He, X.-F. Lu, H. Xu, Y.-X. Tong and G.-R. Li, *Angew. Chem., Int. Ed.*, 2015, **54**, 3669-3673.
8. B. Cai, D. Wen, W. Liu, A. K. Herrmann, A. Benad and A. Eychmuller, *Angew. Chem., Int. Ed.*, 2015, **54**, 13101-13105.
9. W. Wang, Y. Yang, Y. Liu, Z. Zhang, W. Dong and Z. Lei, *J. Power Sources*, 2015, **273**, 631-637.
10. W. Huang, X.-Y. Ma, H. Wang, R. Feng, J. Zhou, P. N. Duchesne, P. Zhang, F. Chen, N. Han, F.

- Zhao, J. Zhou, W.-B. Cai and Y. Li, *Adv. Mater.*, 2017, **29**, 1703057.
11. R. Jana, U. Subbarao and S. C. Peter, *J. Power Sources*, 2016, **301**, 160-169.
 12. X. Yu, Z. Luo, T. Zhang, P. Tang, J. Li, X. Wang, J. Llorca, J. Arbiol, J. Liu and A. Cabot, *Chem. Mater.*, 2020, **32**, 2044-2052.
 13. K. Zhang, D. Bin, B. Yang, C. Wang, F. Ren and Y. Du, *Nanoscale*, 2015, **7**, 12445-12451.
 14. C. Zhu, S. Guo and S. Dong, *Adv. Mater.*, 2012, **24**, 2326-2331.
 15. L. Chen, L. Lu, H. Zhu, Y. Chen, Y. Huang, Y. Li and L. Wang, *Nat. Commun.*, 2017, **8**, 14136.
 16. K. Jiang, P. Wang, S. Guo, X. Zhang, X. Shen, G. Lu, D. Su and X. Huang, *Angew. Chem., Int. Ed.*, 2016, **55**, 9030-9035.
 17. G. Kresse and J. Furthmüller, *Comput. Mater. Sci.*, 1996, **6**, 15-50.
 18. P. E. Blöchl, O. Jepsen and O. K. Andersen, *Phys. Rev. B*, 1994, **49**, 16223-16233.
 19. M. Methfessel and A. T. Paxton, *Phys. Rev. B*, 1989, **40**, 3616-3621.
 20. S. R. Bahn and K. W. Jacobsen, *Comput. Sci. Eng.*, 2002, **4**, 56-66.
 21. S. Azad, M. Kaltchev, D. Stacchiola, G. Wu and W. T. Tysoe, *J. Phys. Chem. B*, 2000, **104**, 3107-3115.
 22. H. J. Monkhorst and J. D. Pack, *Phys. Rev. B*, 1976, **13**, 5188-5192.
 23. E. Pérez-Gallent, G. Marcandalli, M. C. Figueiredo, F. Calle-Vallejo and M. T. M. Koper, *J. Am. Chem. Soc.*, 2017, **139**, 16412-16419.
 24. I. Ledezma-Yanez, E. P. Gallent, M. T. M. Koper and F. Calle-Vallejo, *Catal. Today*, 2016, **262**, 90-94.
 25. F. Calle-Vallejo and M. T. M. Koper, *Angew. Chem., Int. Ed.*, 2013, **52**, 7282-7285.